Proceeding of the 2015 International Conference on Space Science and Communication (IconSpace), 10-12 August 2015, Langkawi, Malaysia

Mathematical Investigations of Gas Flare Constituents in Oil Producing Regions of Malaysia.

T.V. Omotosho[1], M.E. Emetere[2], M.L. Akinyemi[3], M. Abdullah[4], Jit .S, Mandeep[5]
[1, 2, 3]Department of Physics, Covenant University Ota, Ogun State Nigeria
[4, 5]Department of Electrical, Electronic and System Engineering
[4, 5]Space Science Center
Universiti Kebangsaan Malaysia
43600 Bangi, Selangor, Malaysia
[1]omotosho@covenantuniversity.edu.ng, [2]moses.emetere@covenantuniversity.edu.ng,
[3]Marvel.akinyemi@covenantuniversity.edu.ng, [4]mardina@eng.ukm.my, [5]mandeep@eng.ukm.my

***Abstract*—Air pollution due to gas–flaring is a major concern in most region of the world. The short and long term effect of the massive air pollution on the life form within the area requires urgent attention because of the health implication. This research examines the impact of air pollutants in oil producing region of Malaysia using remotely sensed satellite data. The satellite data set was obtained from CALIPSO, MODIS and AIRS. A mathematical software (MATLAB) was used to analyse the results. For Sulphur dioxide (SO2), Kemaman had the highest rate of pollution (0.075DU), then Petronas (0.074DU), Kertih (0.067 DU), Port (0.065DU), Rapids (0.052DU), Melaka 1 (0.032DU) respectively. For Carbon dioxide (CO2), Kertih and Petronas was the most polluted with (382.33ppmv), Melaka 1 and Port had (382.27ppmv), Rapid had (382.04ppmv) and Kemaman (381.53ppmv) respectively. For Nitrogen dioxide (NO2), Petronas had the highest mean value with (311.18mol/cm2), Melaka 1 (243.4mol/cm2), Port (201.5mol/cm2), Rapids (183.3mol/cm2), Kertih (117.73mol/cm2), Kemaman (95.7mol/cm2) respectively. For Ozone (O3), the stations with the highest rate of concentration were Rapids, Melaka 1, Petronas, Kertih and Kemaman with (252.43E+2mol/cm2). Mathematical projections were made to capture the dilemma- people in this region might encounter in the nearest future.**

Keywords-gas flaring; mathematical model; aerosols; Malaysian oil region; greenhouse gase;, aerosol; sulphate; methane; carbon dioxide; nitrate oxide.

I. INTRODUCTION

Gas-flaring emissions like other kind of anthropogenic emissions contribute significantly to global warming, climate change and health deterioration of life-forms if not controlled [1-3]. Gas flares are composed of green gases and aerosols such as sulfur dioxide, oxides of carbon i.e. CO or CO2, nitrogen dioxides, methane, benzapryene, toluene, xylene, and hydrogen sulfide. Unarguably, the steady emission of gas flares into the oil producing region for the past twenty years should attract high volume of pollutants in the planetary boundary layer. Although this initiates unstable precipitations, the possibility of acidic or basic rainfall within the region is inevitable [4]. In 1999, the control of gas flares in Malaysia was prevalent in the 'Kyoto protocol' [5]. The 'Kyoto protocol' was originally designed to mitigate gas flaring by 2008. Six years after (2014), what has been the progress of the 'Kyoto protocol'. Hence in this research, mathematical models shall be used to estimate the various tuning constants which express either a progression or retrogression in the campaign against gas flares in Malaysia. The remote sensing option is a better option to capture the amount of gas flares ejected into the atmosphere per time. The satellite data used for this research were generated from the Giovanni NASA satellite database. Giovanni is a tool that displays Earth science data from NASA satellites directly on the Internet. Giovanni is an acronym for the Goddard Earth Sciences Data and Information Services Center, or GES DISC, Interactive Online Visualization and Analysis Infrastructure. Various data can be generated on Giovanni i.e. atmospheric chemistry, atmospheric temperature, water vapor and clouds, atmospheric aerosols, precipitation, and ocean chlorophyll, surface temperature e.t.c. Basic analytical functions performed by Giovanni currently are carried out by the Grid Analysis and Display System (GrADS). Giovanni supports multiple data formats including Hierarchical Data Format (HDF), HDF-EOS, network Common Data Form (netCDF), GRIdded Binary (GRIB), and binary, and multiple plot types including area, time, Hovmoller, and image animation [6].

A comprehensive mathematical model for both predictive and proactive study of air pollution has been proposed and applied [1-2]. 'A model is not only a substitute of the actual system, it also the simplification of the system' [7]. A plume model can be any of the following, physical static model, physical dynamic model, mathematical static model, mathematical dynamic model, mathematical static analytical model, mathematical dynamic numerical model e.t.c. In this paper we analyze the results obtained from the oil producing region of Malaysia and relate it to a dispersive semi plume model.

II. THEORETICAL DERIVATIONS

The oil producing region of Malaysia is described in figure (1) below. The number of oil exploration point-contributing to gas flaring cannot be ascertained for security reasons, However, we made few reasonable assumptions to suffice for the likely errors during the formulation of the model.

Figure 1: Geographical location of the Gas Flares region

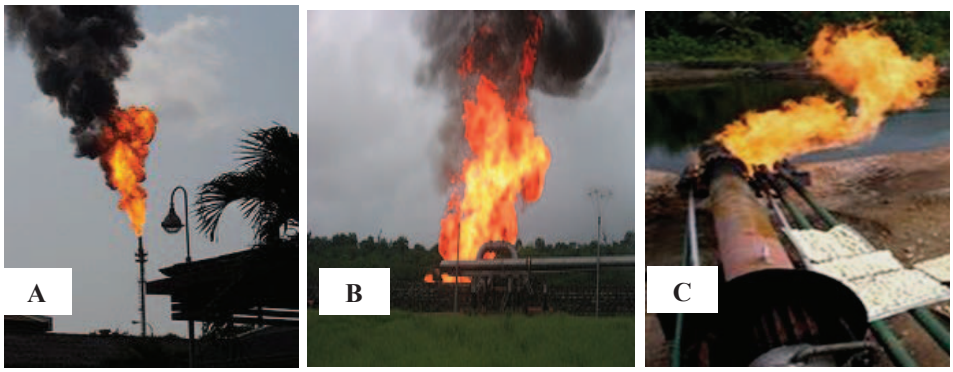

Figure 2A-C: Types of gas flare dispersion. (http://www.foe.org/gas-flaring-nigeria)

Figure 2A is the vertical dispersion method, figure 2B is the scattered dispersion method and figure 2C is the horizontal dispersion method. The full analysis of all the methods had been established [1,2]. The following assumptions were adopted.

1. Inclusion of the mild diffusion at the downwind plane as shown in figure 2A-C. Therefore the measurement of the eddy diffusivity is between 2 -3 m2/s , though it varies from place to place.
2. The angle of deviation (α & β) depends on the wind convection and it does not exceeds the angles. Therefore the gas flares noticed around the stack is as a result of the particulate gas flare splash from the lower turbulent diffusion as shown in figure (3)
3. The presence of air upthrust and air viscosity was made negligible because of the influence of the ground heat flux [8-11].
4. The width of the plume depends on both the wind direction and coefficient of eddy diffusivity.

direction and coefficient of eddy diffusivity.

5. The gas flare particulate is uniformly distributed along the sampling site.
6. The wind speed ranges 1ms-1 and 0.72ms-1 at 10m above the ground (below the planetary boundary layer) during the dry and wet seasons respectively

The pictorial view of particulate dispersion (figure 3) served as the control guide for this model. The model incorporates four equations i.e. general dispersion equation, mild dispersion equation, turbulent dispersion equation and particulate deposition equation. The mild dispersion equation and turbulent dispersion equation applies to any dispersion methods. However, the mild dispersion model is considered in this study because it solves the tropospheric gas transport [1]. Air particles at the mild dispersion region is the lightest by mass and energetic to interact with atmospheric current [12,13].

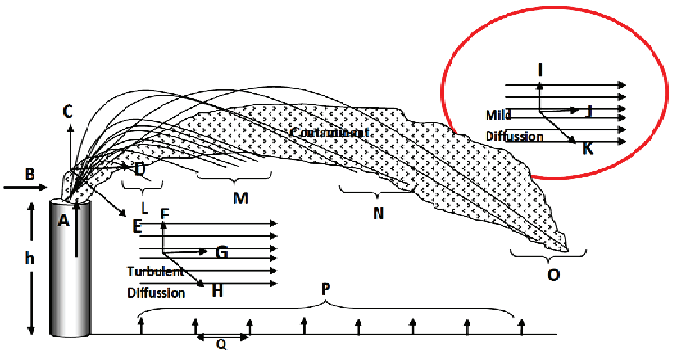

Figure 3: Pictorial analysis of the general dispersion

Figure (3) expresses the different perspectives of the advection diffusion equations adopted for this model was derived. The mathematical expressions for the different positions are mathematically represented below.
Region A-E is the general particulate dispersion analysis

$$\left.\begin{aligned} A = \frac{\partial C}{\partial t}\ ; \quad B = V\frac{\partial C}{\partial r}\ ; \quad C = V_z\frac{\partial C}{\partial z}\ ; \quad D = V_x\frac{\partial C}{\partial x}\ ; \\ E = V_y\frac{\partial C}{\partial y}\ \end{aligned}\right\} \tag{1}$$

Where $V^2 = {V_x}^2 + {V_y}^2 + {V_z}^2$

Region F-H is the turbulent particulate dispersion analysis

$$F = \frac{\partial}{\partial z}\left(K_z\frac{\partial C}{\partial z}\right);\ G = \frac{\partial}{\partial x}\left(K_z\frac{\partial C}{\partial x}\right) = 0;\ H = \frac{\partial}{\partial y}\left(K_y\frac{\partial C}{\partial y}\right) \tag{2}$$

Region I-K is the mild particulate dispersion analysis

$$I = \frac{\partial}{\partial z}\left(K_{z2}\frac{\partial C}{\partial z}\right);\ = \frac{\partial}{\partial x}\left(K_{z2}\frac{\partial C}{\partial x}\right) = 0\ ;K = \frac{\partial}{\partial y}\left(K_{y2}\frac{\partial C}{\partial y}\right); \tag{3}$$

Region L-O is the particulate deposition analysis

$$\left.L \approx \frac{2V_{1x}^3V_y}{gV^2}\ ;\ M \approx \frac{2V_{2x}^3V_y}{gV^2}\ ; \approx \frac{2V_{3x}^3V_y}{gV^2}\ ;\ O \approx \frac{2V_{4x}^3V_y}{gV^2}\right\} \tag{4}$$

V is the wind velocity (m/s), P is the Air Upthrust, C(x,y,z) is the mean concentration of diffusing pollutants of diffusing substance at a point (x,y,z) [kg/m3], Ky, Kx is the eddy diffusivities in the direction of the y- and z- axes [m2/s] and S is the source/sink term [kg/m3-s]
The governing equations are written as

$$\frac{\partial C}{\partial t} + V_x\frac{\partial C}{\partial x} - V_z\frac{\partial C}{\partial z} - V_y\frac{\partial C}{\partial y} = \frac{\partial}{\partial z}\left(K_z\frac{\partial C}{\partial z}\right) + \frac{\partial}{\partial y}\left(K_y\frac{\partial C}{\partial y}\right) + \frac{\partial}{\partial z}\left(K_{z2}\frac{\partial C}{\partial z}\right) + \frac{\partial}{\partial y}\left(K_{y2}\frac{\partial C}{\partial y}\right) - P + S \tag{5}$$

$$V_z\frac{\partial C}{\partial z} = \frac{\partial}{\partial z}\left(K_z\frac{\partial C}{\partial z}\right) + \frac{\partial}{\partial y}\left(K_y\frac{\partial C}{\partial y}\right) + \frac{\partial}{\partial x}\left(K_z\frac{\partial C}{\partial x}\right) \tag{6}$$

$$V_x\frac{\partial C}{\partial x} = \frac{\partial}{\partial y}\left(K_{y2}\frac{\partial C}{\partial y}\right) + \frac{\partial}{\partial z}\left(K_{z2}\frac{\partial C}{\partial z}\right) + \frac{\partial}{\partial x}\left(K_{z2}\frac{\partial C}{\partial x}\right) \tag{7}$$

Equation (7) is the mild dispersion equation. The mild dispersion equation occurs in two 2D on the account of individual gas molecule transport. It is mathematically expressed as

$$\left.\begin{aligned} V_x\frac{\partial C_1}{\partial x} = \frac{\partial}{\partial y}\left(K_{y2}\frac{\partial C}{\partial y}\right) + \frac{\partial}{\partial z}\left(K_{z2}\frac{\partial C}{\partial z}\right) \\ V_x\frac{\partial C_2}{\partial x} = \frac{\partial}{\partial z}\left(K_{z2}\frac{\partial C}{\partial z}\right) + \frac{\partial}{\partial x}\left(K_{z2}\frac{\partial C}{\partial x}\right) \end{aligned}\right\} \tag{8}$$

Equation (8) is the ascending particulate-mild dispersion equation

$$\left.\begin{aligned} V_x\frac{\partial C_1}{\partial x} = \frac{\partial}{\partial y}\left(K_{y2}\frac{\partial C}{\partial y}\right) - \frac{\partial}{\partial z}\left(K_{z2}\frac{\partial C}{\partial z}\right) \\ V_x\frac{\partial C_2}{\partial x} = -\frac{\partial}{\partial z}\left(K_{z2}\frac{\partial C}{\partial z}\right) + \frac{\partial}{\partial x}\left(K_{z2}\frac{\partial C}{\partial x}\right) \end{aligned}\right\} \tag{9}$$

Equation (9) is the descending particulate-mild dispersion equation
It was solved using separation of variable i.e. C=X(x)Y(y) with the initial boundary condition are x=1, X=1; y=1, Y=1; z=1, Z=1. The solution is given as

$$C(x,y,z) = a^2\mathrm{bcos}\left(\frac{\mathrm{n}}{\mathrm{k_y}} + \alpha\right)\cos\left(\frac{\mathrm{n}}{\mathrm{k_z}} + \beta\right)\exp\left(\frac{n^2}{V_x}\right) \tag{10}$$

a, b, n, α, and β are constants that would be determined via remotely sensed data set. The practical application of equation (10) is explained in the next session.

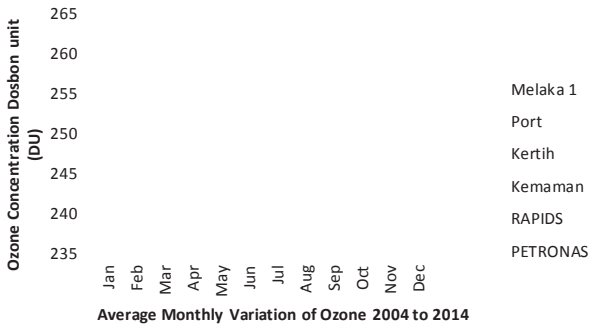

Figure 4a: Ozone satellite analysis from 2004 to 2012

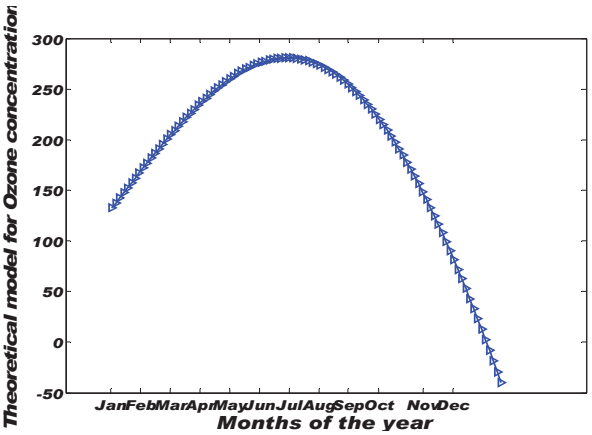

Figure 4b: Ozone satellite analysis from 2004 to 2012

III. RESULTS AND DISCUSSION

The peak of the ozone in the year can be seen in August/September. Generally, the ozone content over the regions are predictable. However, the theoretical simulation reveals the possibility of further reduction expecially in October-February. The values of the tuning constants can be seen in Table 2. The tuning constant gives more precession and accuracy to the automatic weather stations used in the region. The tuning constants are configured into the compact flash(CF) card of the weather station.

For Sulphur dioxide (SO2), Kemaman had the highest rate of pollution (0.075DU), then Petronas (0.074DU), Kertih (0.067 DU), Port (0.065DU), Rapids (0.052DU), Melaka 1 (0.032DU) respectively. For Carbon dioxide (CO2), Kertih and Petronas was the most polluted with (382.33ppmv), Melaka 1 and Port had (382.27ppmv), Rapid had (382.04ppmv) and Kemaman (381.53ppmv) respectively. For Nitrogen dioxide (NO2), Petronas had the highest mean value with (311.18mol/cm2), Melaka 1 (243.4mol/cm2), Port (201.5mol/cm2), Rapids (183.3mol/cm2), Kertih (117.73mol/cm2), Kemaman (95.7mol/cm2) respectively. For Ozone (O3), the stations with the highest rate of pollution were Rapids, Melaka 1, Petronas, Kertih and Kemaman with (252.43E+2mol/cm2). We applied statistical approximation technique to estimate the region of cumulative gas flare threat. The region of highest gas flare threats in descending order are Petronas, Melaka 1, Port, Rapid, Kertih and Kemaman (see Table 1).

The sulphur dioxide content shows maximum of three peaks in a year with the highest value at September (see figure 6). Like the ozone, they both share the same peak trend. This simply means there are possibilities of both gases reacting in a high humid atmosphere as shown in the expression below.

$$4SO_2 + 4O_3 + 4H_2O \rightarrow 4H_2SO_4 + 4O_2$$

There may be possibility of acid rain only if the rain extends into late August. The CO content has its peak around February and November. It also has a drastic fall around June and July (see figure 7). The CO content is slightly predictable.

The CO2 content has its peak around May, June and July. It also has a drastic fall around January and December (see figure 8). The CO content is very slightly predictable. Very significant observation in figure 8 & 9 shows that an inverse relationship exists between the CO and CO2 contents around June and July. Its main difference can be observed in the tuning constants derived for both gases.

NO2 content is the most unpredictable gas in all the regions. Though the NO2 content shows fairly sinusoidal features, the individual NO2 emission differs. Hence, the tuning constants for NO2 content in Malaysia cannot be estimated.

As seen in table 2, SO2 have the highest speed in the Malaysian atmosphere. Its angular displacements are very small. Hence it may not spread like other gases. It has the tendency to go downward whenever precipitation is high. Therefore if gas flaring continues, SO2 has the potential of creating greater damage in all the regions. O3 and CO2 have almost the same characteristics except that its horizontal angular displacement is very small. CO have the lowest speed in the atmosphere. It diffuses into the atmosphere in a slow but steady manner. Unlike SO2, its volume in the atmosphere is not affected by much precipitation. Therefore may be eliminated only after its expiration of its life-time. The glaring peaks noticed in January and February shows the tendency of its mean equilibrium to rise above its current state. SO2 and CO have often stable and shallow atmospheric boundary layer at night-causing the mixing ratio to build up in a thin layer near the surface. During the day, the boundary layer is often convective and deep-causing it to dilute over large vertical extent. It has the tendency to go downward whenever precipitation is high. Therefore if gas flaring continues, SO2 has the potential of creating greater damage to life forms. O3 and CO2 has almost the same characteristics except that its horizontal angular displacement is very small. Against the rectifier effect theory noticed for CO2 [14], the regions do not observe the asymmetric mixing ratio of the rectified CO2..

IV. CONCLUSION

The movement of atmospheric pollution across large land mass is of concern to mankind. Therefore the struggle against the emission of greenhouse gases or aerosols into our environment should not be underestimated. The 'Kyoto protocol' has shown little as more efforts are required to avoid adverse climate change in the regions. Most importantly is that the rectifier effect theory holds for SO2 not CO2.

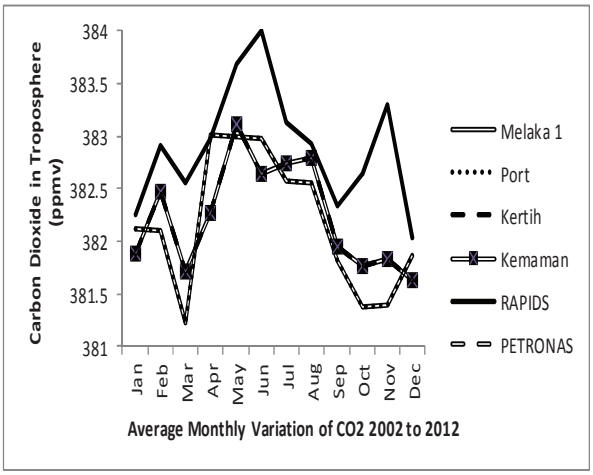

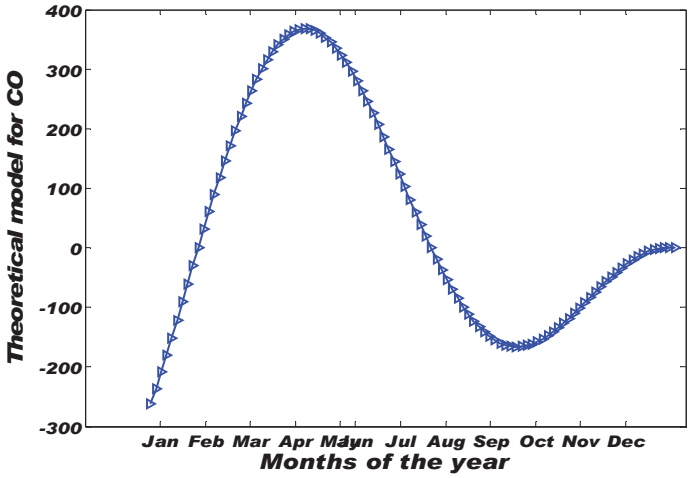

Figure 7: CO2 satellite analysis from 2000 to 2012

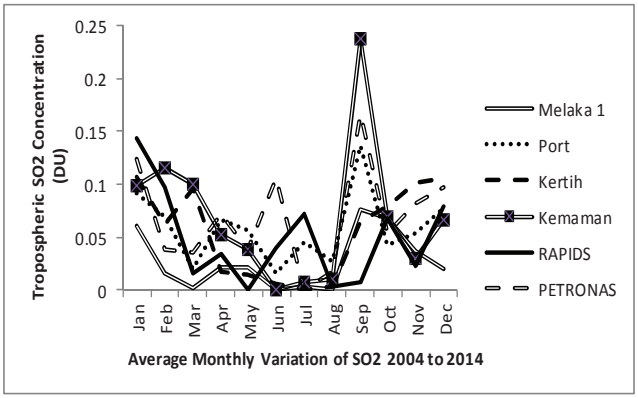

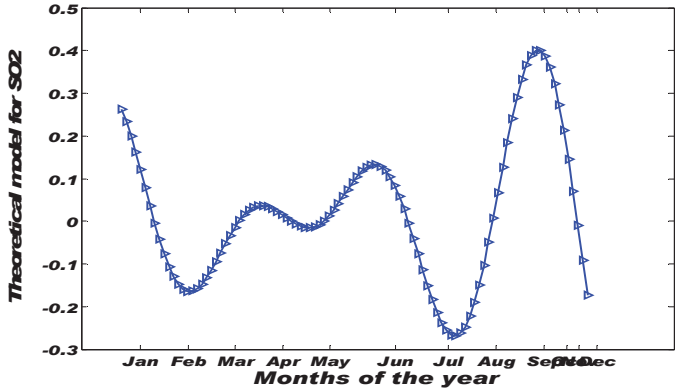

Figure 6: SO_2 satellite analysis from 2004 to 2014

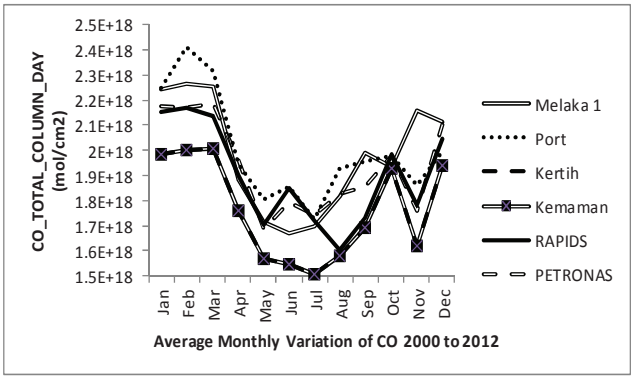

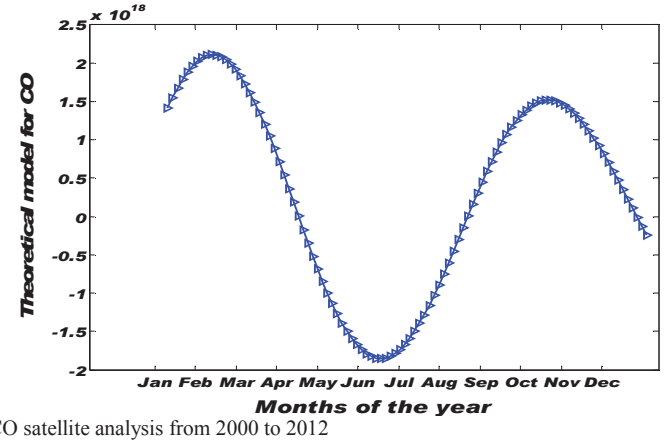

Figure 7: CO satellite analysis from 2000 to 2012

TABLE 1: STATISTICAL DETERMINATION OF GAS FLARES CUMULATIVE EFFECT

	O_3	NO_2	CO_2	SO_2	CO	Total
Melaka 1	5	5	4	1	5	20
Port	1	4	4	3	6	18
Kertih	3	2	5	4	1	15
Kemaman	2	1	1	6	2	16
Rapid	6	3	2	2	3	16
Petronas	4	6	5	5	4	24

TABLE 2: THE DISPERSION PARAMETERS DESCRIBING THE INDIVIDUAL GAS BEHAVIOUR IN THE ATMOSPHERE

Type	$\frac{n^2}{V_x}$	α	β	$\frac{n}{k_{y_{max}}}$	$\frac{n}{k_{z_{max}}}$	$\frac{n}{k_{y_{min}}}$	$\frac{n}{k_{z_{min}}}$	$a = b$
CO_2	6.1	2.5	0.009	$\frac{11}{4}\pi$	$\frac{1}{2}\pi$	$\frac{1}{2}\pi$	$\frac{1}{18}\pi$	1
SO_2	-0.001	0.5	1.2	$\frac{5}{2}\pi$	$-\frac{10}{4}\pi$	$\frac{9}{4}\pi$	$-\frac{16}{2}\pi$	1
O_3	6.65	20.5	1.5	π	$\frac{1}{4}\pi$	$\frac{1}{3}\pi$	$\frac{1}{12}\pi$	1
CO	42.3	4.9	0.2	3π	$\frac{1}{4}\pi$	$\frac{1}{6}\pi$	$\frac{1}{16}\pi$	1

ACKNOWLEDGMENT

The authors acknowledge the Center for Research and Development (CUCRID), Covenant University, Ota, Nigeria for grants to purchase the research equipment.

REFERENCES

[1] Emetere, and M.L Akinyemi, "Modeling Of Generic Air Pollution Dispersion Analysis From Cement Factory". Analele Universitatii din Oradea–Seria Geografie 231123-628, pp181-189, 2013.

[2] Emetere,Moses E. , "Modeling Of Particulate Radionuclide Dispersion And Deposition From A Cement Factory". Annals of Environmental Science,7(6), pp71-77, 2013.

[3] Emetere, M. E., "Theoretical Forecast of the Health Implications of Citing Nuclear Power Plant in Nigeria", Journal of Nuclear and Particle Physics, 4(3), pp87-93,2014

[4] Watts M.(2001). Petroleum violence: communities, extraction and political ecology of a mythic commodity.189-212pp. Cornell University Press

[5] Unknown, http://3greengtl.com.my/pim/flaring-in-malaysia.html, 2009

[6] NASA,http://www.nasa.gov/audience/foreducators/9-12/features/giovanni-an-easier-way.html 2009

[7] Ana, G.R. and E.E. Sridhar, " Industrial Emissions and Health Hazards among selected factoryworkers at Eleme, Nigeria". J. Env. Heal. Res., l9(1), pp43-51, 2009.

[8] Tawari C.C. and J.F.N. Abowei, "Air Pollution in the Niger Delta Area of Nigeria, International". Journal of Fisheries and Aquatic Sciences 1(2), 94-117, 2012

[9] Dinesh K. S., "Modelling Cyber-security". International Journal of Applied Physics and Mathematics, 2 (5), pp312-315, 2012

[10] Uno EU, Emetere M E. "Analysing the Impact of Soil Parameters on the Sensible Heat Flux Using Simulated Temperature Curve Model". International Journal of Physics & Research, 2, pp1-9, 2012

[11] Uno EU, Emetere ME, Eneh C D. "Simulated Analysis of soil heat flux using temperature deviation model". Science Journal of Physics, 2012, pp1-9, 2012

[12] Lovejoy ER, Curtius J, Froyd KD. "Atmospheric ion-induced nucleation of sulphuric acid and water", Journal of Geophysical Research, 2004, 109: D08204.

[13] de Gouw JA, Warneke C, Stohl A, Wollny AG, Brock CA, Cooper OR, Holloway JS, Trainer M. "Volatile organic compounds composition of merged and aged forest fire plumes from Alaska and western Canada", Journal of Geophysical Research, 2006,111: D10303.

[14] Larson V.E., & Volkmer H. An idealized model of the one dimensional carbon dioxide rectifier effect. Tellus B, 2008, 20: 525-536.